THE JOURNAL OF BIOLOGICAL CHEMISTRY
Vol. 280, No. 15, Issue of April 15, pp. 14865–14876, 2005

Printed in U.S.A.

Structural Mechanism Governing the Quaternary Organization of Monocot Mannose-binding Lectin Revealed by the Novel Monomeric Structure of an Orchid Lectin*

Received for publication, October 13, 2004, and in revised form, January 11, 2005
Published, JBC Papers in Press, January 13, 2005, DOI 10.1074/jbc.M411634200

Wei Liu‡§, Na Yang‡§¶, Jingjin Ding‡¶, Ren-huai Huang‡, Zhong Hu‖, and Da-Cheng Wang‡**

From the ‡Center for Structural and Molecular Biology, Institute of Biophysics, Chinese Academy of Sciences, Beijing 100101, ¶Graduate School of Chinese Academy of Sciences, Beijing 100039, and ‖Kunming Institute of Botany, Chinese Academy of Sciences, Kunming 650204, People's Republic of China

Two isoforms of an antifungal protein, gastrodianin, were isolated from two subspecies of the orchid *Gastrodia elata*, belonging to the protein superfamily of monocot mannose-specific lectins. In the context that all available structures in this superfamily are oligomers so far, the crystal structures of the orchid lectins, both at 2.0 Å, revealed a novel monomeric structure. It resulted from the rearrangement of the C-terminal peptide inclusive of the 12th β-strand, which changes from the "C-terminal exchange" into a "C-terminal self-assembly" mode. Thus, the overall tertiary scaffold is stabilized with an intramolecular β-sheet instead of the hybrid observed on subunit/subunit interface in all known homologous dimeric or tetrameric lectins. In contrast to the constrained extended conformation with a *cis* peptide bond between residues 98 and 99 commonly occurring in oligomers, a β-hairpin forms from position 97 to 101 with a normal *trans* peptide bond at the corresponding site in gastrodianin, which determines the topology of the C-terminal peptide and thereby its unique fold pattern. Sequence and structure comparison shows that residue replacement and insertion at the position where the β-hairpin occurs in association with *cis-trans* interconversion of the specific peptide bond (97–98) are possibly responsible for such a radical structure switch between monomers and oligomers. Moreover, this seems to be a common melody controlling the quaternary states among bulb lectins through studies on sequence alignment. The observations revealed a structural mechanism by which the quaternary organization of monocot mannose binding lectins could be governed. The mutation experiment performed on maltose-binding protein-gastrodianin fusion protein followed by a few biochemical detections provides direct evidence to support this conclusion. Potential carbohydrate recognition sites and biological implications of the orchid lectin based on its monomeric state are also discussed in this paper.

Plant lectins are defined as proteins possessing at least one non-catalytic domain that binds reversibly to a specific mono- or oligosaccharide (1). Because of the increasing availability of sequence and structure information, the majority of all known plant lectins have been recently subdivided into seven structural and evolutional related groups (2). Among these classes are monocot mannose-binding lectins that preferably bind to 1–3- or 1–6-linked D-mannoses with the highest affinity (3). Lectins from this protein superfamily having been isolated and characterized so far come from Amaryllidaceae, Alliaceae, Araceae, Liliaceae, Orchidaceae, and recently reported Iridaceae families (2, 4). All these proteins are found to present three potential carbohydrate binding motifs per subunit, each of which contains a consensus sequence signature Q*X*DXN*X*-V*XY*, essential for mannose binding (5).

All currently known monocot mannose binding lectins with available three-dimensional structures in the Protein Data Bank are hololectins built from two or four identical one-domain promoters. It has been widely believed that oligomerization and multivalency thereby play an important role in variability of carbohydrate recognition among plant lectins. For instance, tetrameric proteins such as snowdrop and daffodil lectins bind with mannan epitopes on GP120, the major glycoprotein of human immunodeficiency virus, with a high degree of affinity (6, 7), whereas garlic agglutinin, a dimer, does not (8, 9). *Galanthus nivalis* agglutinin (GNA)[1] from snowdrop bulbs was the first member of this protein superfamily to have its crystal structure determined (10), and since then, a series tetrameric or dimeric structures of monocot lectins from amaryllis (*Hippeatrum* hybrid) (11), bluebell (*Scilla campanulata*) (12), daffodil (*Narcissus pseudonarcissus*) (13), and garlic (*Allium sativum*) (14, 15) have been reported as well as a two-domain lectin from *S. campanulata* (16).

The basic structural unit for bulb lectins is a dimer, as revealed in the cited literature. In all the studied structures two subunits are related by a pseudo-2-fold symmetry axis and assemble into a tightly bound dimer by exchanging their C-terminal β-strands (residues 101–105 in GNA) to form a hybrid β-sheet (10). This mode often referred to as the C-terminal exchange confers a large buried area on the subunit/subunit interface through which a stable dimer is established. An unusual *cis* peptide bond between Gly-98 and Thr-99 is commonly involved in those oligomers and believed to play a vital role for strand exchange (10, 12, 13). From an energetic and structural point of view, monomers cannot exist stably when a dimer dissociates, as expected and verified calorimetrically (17). How-

* The work was supported by National Natural Science Foundation of China (NSFC Grant 30070162) Ministry of Sciences and Technology of China Grants 863-2002BA711A13 and 973-G1999075064, and Chinese Academy of Sciences (Grants KSCX1-SW-17 and KSCX2-SW-322). The costs of publication of this article were defrayed in part by the payment of page charges. This article must therefore be hereby marked "*advertisement*" in accordance with 18 U.S.C. Section 1734 solely to indicate this fact.

The atomic coordinates and structure factors (codes 1XD5 (gastrodianin-1) and 1XD6 (gastrodianin-4)) have been deposited in the Protein Data Bank, Research Collaboratory for Structural Bioinformatics, Rutgers University, New Brunswick, NJ (http://www.rcsb.org/).

§ Both authors contributed equally to this work.

** To whom correspondence should be addressed. Tel.: 86-10-64888547; Fax: 86-10-64888560; E-mail: dcwang@sun5.ibp.ac.cn.

[1] The abbreviations used are: GNA, *G. nivalis* agglutinin; MBP, maltose-binding protein; r.m.s.d., root mean square (r.m.s.) deviation.

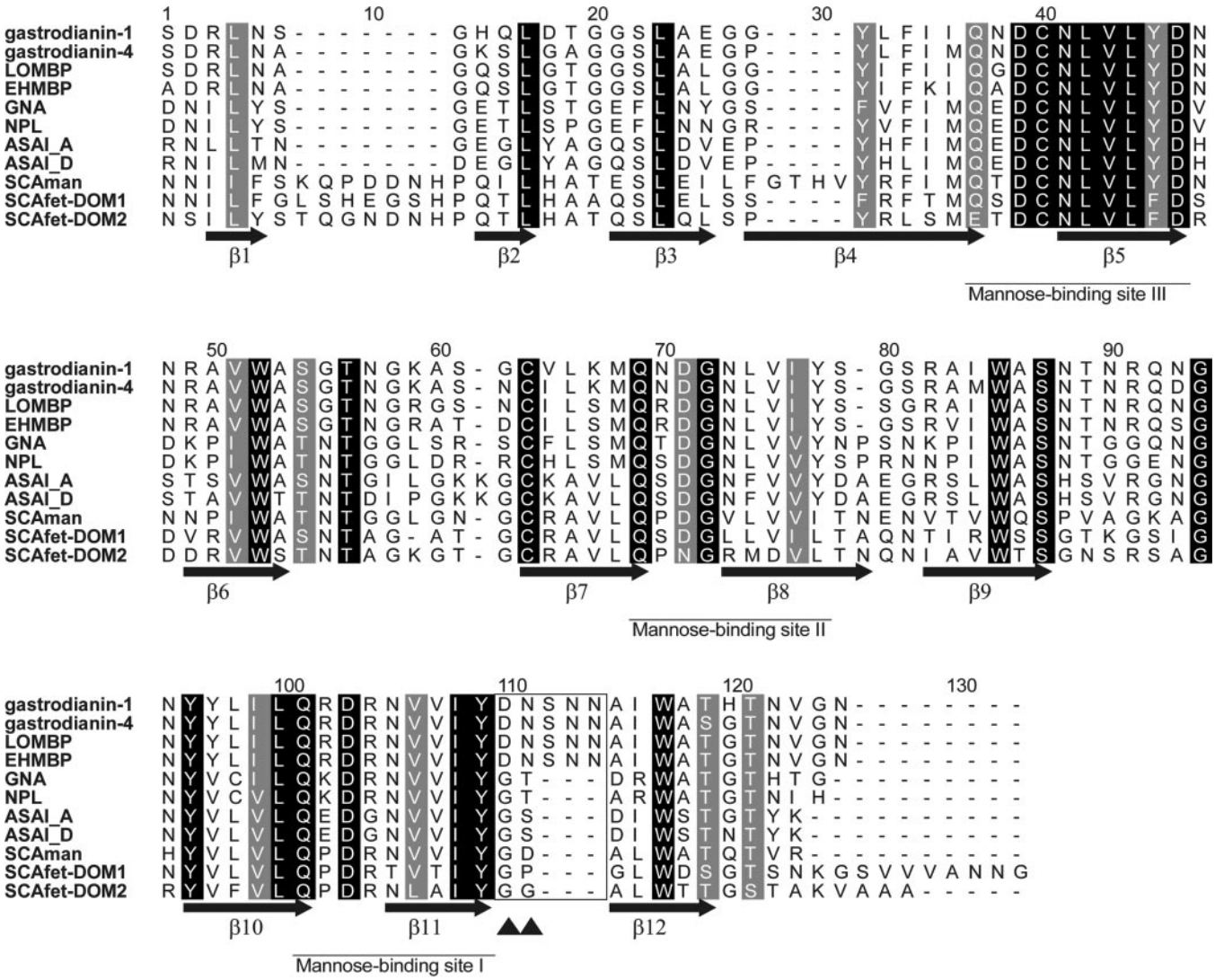

FIG. 1. **Sequence alignment among gastrodianin-1, gastrodianin-4, and their homologies inclusive of *L. ovata* mannose-binding protein (*LOMBP*), *E. helleborine* mannose-binding protein (*EHMBP*) (19), GNA (10), *N. pseudonarcissus* lectin (*NPL*) (13), subunits A and D from *A. sativum* agglutinin (15), SCAman (12), and domains 1 and 2 of SCAfet (16).** The residue positions are *numbered* in terms of gastrodianin. All identities and similarities are *shaded* with a *dark background*, and the β-barrel-related strands are labeled with *arrows* beneath the sequence. All three mannose-binding sites with the consensus sequence motif are marked in the alignment, and the two residues at positions 97 and 98 (corresponding to 98 and 99 for GNA or *N. pseudonarcissus* lectin), where a *trans* peptide bond is present in between monomers instead of the *cis* peptide bond generally existing in oligomers, are denoted with up-triangles.

ever, three merolectins containing a single protomer have already been isolated and sequenced from Orchidaceae, *i.e. Lister ovata* and *Epipactis helleborine* (18, 19) and *Gastrodia elata* (20). In this context it would be of great interest to uncover unique structural features of these monomers different from those presented in oligomers for the purpose of gaining deeper insight into structural mechanisms governing the quaternary association for monocot mannose-binding lectins.

Gastrodianin, also known as *Gastrodia* antifungal protein (GAFP) previously, is purified from the nutritive corms of the orchid *G. elata*, a traditional Chinese medicinal herb cultured for thousands of years. The plant lacks chlorophyll and leads a parasitic life on the fungus *Armillaria mellea*. The fungal hyphae invade the nutritive and the primary corm of *G. elata* during its development. The cortical cells in corms, however, capture and digest the infecting hyphae and transport the released nutrients into a terminal corm for sustaining its growth (21). Histochemical localization studies *in vivo* showed that a mannose-binding lectin, later named gastrodianin, accumulates in nutritive corms where fungal infection takes place (20, 22). Antifungal assays *in vitro* also confirmed a strong inhibitive activity of gastrodianin toward a wide range of phytopathogenic fungi, such as *Trichoderma viride*, *Valsa ambiens, Rhizoctonia solani, Gibberella zeae, Ganoderma lucidum*, and *Botrytis cinerea* (23). As a common phenomenon a number of isolectins simultaneously occur in one plant, and several isoforms have been identified from *G. elata*, differing subtly from each other in their sequence. At least five of them have been distinguished on the level of cDNA sequences (24–26). The mature protein is estimated to be 112 amino acids long and behaves as a monomer in solution (25). Sequence alignment (Fig. 1) indicates that gastrodianins belong to the superfamily of monocot lectins and share the highest degree of identity with two other orchid merolectins, *L. ovata* and *E. helleborine* mannose-binding proteins (18).

We report here the native crystal structures of two gastrodianin isoforms purified from two subspecies of *G. elata* named gastrodianin-1 and gastrodianin-4 according to their cDNA numbers. With a background of a plethora of attention given to oligomeric plant lectins, the refined structures of gastrodianin

provide us with a scientific glimpse of a monomeric mannose-binding lectin for the first time. It also reveals a potential structural mechanisms governing protein assembly in this superfamily, with possible links to their biological roles in the plant. Furthermore, the conclusion from the structural analysis was generally confirmed by mutagenesis experiments on recombinant maltose-binding protein (MBP)-gastrodianin fusion protein.

MATERIALS AND METHODS

Purification and Crystallization—Gastrodianin-1 and gastrodianin-4 were isolated from newborn terminal corms of two subspecies of the orchids, namely *G. elata* B1 *f. elata* and *G. elata* B1 *f. glauca*, respectively. The purification and crystallization of gastrodianin-1 have been described previously (27), and an identical scheme was applied on gastrodianin-4. The only difference in crystallization trials between the two proteins was the different additives used; that is, 2.5% of dioxane for gastrodianin-1 and 3~5% m-phenylenediamene for gastrodianin-4. Both crystals underwent a long period of growth before shooting.

Data Collection—Data collection, processing, and preliminary analysis for gastrodianin-1 were carried out as described previously (27). A 2.0-Å data set for gastrodianin-4 was collected at room temperature on the beamline of BL-6B at the Photon Factory in KEK, Tsukaba, Japan, with a synchrotron radiation source. X-ray diffraction patterns were record on a Weissenberg camera. Evaluation and scaling of intensity data were processed using DENZO and SCALEPACK in HKL program package (28). The completeness of the whole data sets reached 95.3%.

Structure Determination—The structure solution for gastrodianin-4 was first achieved by a molecular replacement technique using the program AMoRe (29), with a search probe constructed on a truncated model of subunit C of GNA (PDB code 1MSA (10)) without the 11 residues at the C terminus. A reasonable R-factor of 40.8% and a correlation coefficient of 60.7% were given from the top solution after rigid body refinement. In the case of gastrodianin-1, four molecules were estimated in an asymmetric unit of the crystal (27), and the program MOLREP (30) in the CCP4 program suite (31) was used instead of AMoRe with the refined model of gastrodianin-4 as the search probe. The correlation factor rose from 25.7 to 58.5% in four cycles, whereas the R-factor went down from 55.1 to 41.3%. Very few close contacts indicated that the final combined coordinates from MOLREP were acceptable.

Model Building and Refinement—Although a truncated search model from a subunit of snowdrop lectin was used in molecular replacement, extra electron densities were clearly present at the C terminus, accommodating additional residues beyond residue 98. Proper residues in accordance with the sequence were manually fitted one by one into the density map with the program O (32), and several rounds of positional refinement were needed at intervals to improve map quality.

After the completion of model building at the C terminus and the replacement of all various residues that differ between gastrodianin and GNA, the final models from molecular replacement for both orchid lectins were refined by simulated annealing at the initial stages followed by energy minimization with the CNS program suite (33) and with REFMAC (34) at the final round. Anisotropic scaling for initial B factor and solvent contribution was included in the process of refinement with both CNS and REFMAC. The thermal parameters were refined on individual atoms.

Non-crystallographic symmetry restraints were applied between four monomers in the gastrodianin-1 structure during the first simulated annealing runs to prevent over-refinement but with decreasing *Wa* (Non-crystallographic symmetry restraint weight) from cycle to cycle until the last rounds of refinement when neither positional nor B-factor restraints were applied. This allowed for conformational variability among monomers. In both cases solvent molecules as well as sulfate ions were incorporated when the polypeptides became stable until no significant feature remained in the difference map. The occupancy of sulfate ions was refined within a reasonable range of thermal factor. The agreement between the atomic models and x-ray data was checked by SFCHECK (35), and proper geometries were verified using PROCHECK (36).

Expression of MBP-Gastrodianin Fusion Protein—Because of the unavailability of soluble recombinant gastrodianin from various expression systems including *Escherichia coli* and yeast, oligomeric studies had to be performed with resorting to fusion protein expression. The cDNA encoding gastrodianin-1 was obtained from the topical corm of *G. elata* B1 *elata* using 3′-rapid amplification of cDNA ends as reported previously (24). A nucleotide sequence corresponding to the mature lectin from residue 1 to 112 was inserted into pMAL-p2 (New England Biolabs), downstream of the gene encoding the MBP, following the protocol described by Wang *et al.* (25). MBP-gastrodianin fusion protein was produced in *E. coli* host strain TB1 and purified through affinity chromatography on a column packed with amylose resin (New England Biolabs) in the first step. The fraction of interest was subsequently concentrated with ultrafiltration (Millipore) and then loaded onto a Superdex 75 10/300 GL column (Amersham Biosciences) preequilibrated with 50 mM phosphate buffer, pH 7.0, and 0.15 M NaCl at room temperature.

Mutation Experiments—To confirm the conclusion from the structure analysis, the mutation from Asp-97—Asn-98—Ser-99—Asn-100—Asn-101—Ala-102—Ile-103 into Gly-97—Thr-98—Asp-99—Arg-100 on the loop sequence of gastrodianin gene was fulfilled by multiple-round PCR. Four mutagenic primers were synthesized for the purpose of stepwise nested amplification. A pair of primers, 5′-primer (5′-TCAGATCGGTTGAATTCGGGC-3′) and one of 3′-primers (primer 1, 5′-ACGGTCAGTACCGTATATGACGACGTTACGATC-3′; primer 2, 5′-ATTTCCAACGTTGGTGTGGGTTGCCCAACGGGTCAGTACCGTATATGAC-3′; primer 3, 5′-GTGGGATCCATTAATTTCCAACGTTGGTGTGGG-3′) was applied for each run in sequence, and the intermediate amplified product was used as the PCR template for the following round after purification from agarose gel. DNA sequencing was preformed to guarantee the correctness of the final mutant gene. The expression and purification of the mutant fusion protein were carried out with the same protocol as that for the wild type.

Detection of Oligomerization—Oligomerization of the mutant MBP-gastrodianin fusion protein was detected by the following experiments with the wild type fusion protein used as the control. First, the wild and mutant proteins were comparatively analyzed by gel filtration chromatography on Hiload 16/60 Superdex 75 column. The molecular size of wild and mutant fusion proteins were then measured by using a Superdex 75 column (separation range from 3,000 to 70,000) and a Superdex 200 10/300 HR column (separation range from 10,000 to 600,000) (Amersham Biosciences). The two columns were calibrated with low and high M_r protein standard kits, respectively, the former comprising ribonuclease A (M_r 13.7), chymotrypsinogen A (M_r 25.0), ovalbumin(M_r 43.0) and bovine serum albumin (M_r 67.0), and the latter including aldolase (M_r 158), catalase (M_r 232), ferritin (M_r 440), and thyroglobulin (M_r 690). The elution solution used in the experiments contained 0.15 M NaCl in 50 mM phosphate buffer, pH 7.0, which was eluted at the flow rate of 0.5 ml/min.

RESULTS AND DISCUSSION

Quality of Model—Both structures determined by molecular replacement and refined at 2.0 Å resolution showed acceptable values of either crystallographic or free R-factors. Reasonable r.m.s. statistics concerning bond length and angles indicated the stereochemical correctness of the final coordinates. All the relative data are listed in Table I.

Four molecules of gastrodianin-1, named A, B, C, and D, resided in the asymmetric unit and behaved somewhat dissimilarly during refinement. High quality electron density accommodated all 112 amino acids for monomer A and B, whereas one or two residues of C and D were missing due to the lack of density at their C termini. Molecules A and B both have far lower averaged B-factors than those of C or D as a result of more stabilizing contacts from neighboring molecules. Two disordered loop regions 45–52 and 77–82 of molecule D, which protrude from molecular surface into solvent, are poorly defined in the $2F_o - F_c$ map.

Given the different packing mode, the crystal structure of gastrodianin-4 contained only one molecule in the asymmetric unit belonging to a different space group (Table I). The model of gastrodianin-4 was refined to a little higher R-factor and has a lower degree of precision than gastrodianin-1, ascribed from higher solvent content and fewer stabilizing contacts among protein chains. Still, the loop region 45–52 is stabilized through a lattice contact, whereas the loop 77–82 keeps disorder, and the density for two residues at the C terminus is missing.

C Terminus—Bulb lectins are believed to undergo a post-translational modification during maturation. As for gastrodi-

TABLE I
Data processing and refinement statistics

	Gastrodianin-1	Gastrodianin-4
Crystal		
Space group	$P2_12_12$ (No. 18)	$C222_1$ (No. 20)
Unit cell dimensions (Å)	a = 61.1, b = 91.5, c = 81.1	a = 78.1, b = 97.5, c = 36.1
Contents of the asymmetric unit	4 monomers (A and B,112 residues; C, 111 residues; D, 110 residues)	1 monomer (110 residues)
Data collection		
No. of unique reflections	31,377	9,216
Redundancy	6.23	
Resolution range (Å) (last shell)	24.69-2.0 (2.11-2.0)	18.93-2.0 (2.07-2.0)
Completeness (%) (last shell)	99.8 (99.8)	95.3 (91.2)
I/σ (last shell)	6.7 (2.5)	6.3 (2.9)
R_{merge} (%) (last shell)	9.7 (29.6)	6.7
Refinement		
Reflections used in refinement	31,339	9,092
Size of test set (%)	5.0	7.5
R_{cryst}/R_{free} (%)	16.6/20.6	19.9/23.8
Ramachandran plot		
Core region (%)	84.9	88.5
Allowed region (%)	15.1	10.5
Model		
No. of protein atoms	3,442	847
No. of hetero atoms	10	5
No. of solvent molecules	265	43
r.m.s.d. of bond lengths (Å)	0.008	0.010
r.m.s.d. of bond angles (degree)	1.29	1.45
r.m.s.d. of dihedral angles (degree)	27.11	27.66
r.m.s.d. of improper angles (degree)	1.18	1.31
Estimated coordinate error (Å)[a]	0.189/0.183	0.244/0.194
Averaged B-factors (Å^2)		
Protein atoms	Monomer A, 13.6 Monomer B, 14.1 Monomer C, 22.5 Monomer D, 27.0	24.7
Hetero atoms	17.1	33.0
Solvent atoms	31.1	38.2

[a] Estimated according to a Luzzati plot (54) and the Cruickshank method (55).

anin, even if the cDNA sequences corresponds to a 171-amino acid pre-polypeptide, the precise cleavage site at the C terminus is still in debate (24, 25). The same pending problems were left on other orchid lectins inclusive of *L. ovata* mannose-binding protein and *E. helleborine* mannose-binding protein as well, both of which were thought to exist as monomers (19). In the final model of gastrodianin-1, the C termini of two monomers (A and B) can be clearly traced in the density map because they are strongly fixed by neighboring monomers (D and C respectively) via salt bridges from their N-terminal cationic groups. In this case definite electron densities reasonably account for the presence of the carboxyl group at Asn-112 as the last residue of the chain (Fig. 2). We thereby identified that the mature gastrodianin is comprised of 112 residues as the total length and could even presume that the mature peptides of *L. ovata* mannose-binding protein and *E. helleborine* mannose-binding protein are also composed of 112 amino acids since the sequence identity among them reaches as high as 83% (Fig. 1).

Overall Structure of Gastrodianin—The four crystallographic independent molecules of gastrodianin-1 form two pseudo-dimers (AD and BC) in the asymmetric unit, which related by a non-crystallographic 2-fold axis almost parallel to the y axis (179.36°) (Fig. 3*a*). Seven hydrogen bonds between A and D or B and C and two salt bridges between A and B are involved in stabilizing intermolecular contacts (Fig. 3*b*). In the crystallographic lattice of gastrodianin-4, a number of hydrogen bonds are involved in contacts between symmetric related molecules, among which Asn-36 is supposed to be most notable. Both main chain and the side chain of the residue contribute to interactions with neighboring molecules, and very probably for this reason, its dihedral angles fall in the disallowed region of the Ramachandran plot, as is often observed in the oligomeric structures of bulb lectins (12, 13). Least-square superpositions of main chain atoms among all independent molecules in the gatrodianin-1 structure give r.m.s differences ranging from 0.27 Å (A-B) to 0.43 Å (A-D) and r.m.s. differences of 0.51 Å between the two isolectins, gastrodiannin-1 and gastrodianin-4, indicating absolute structural consensus among these molecules despite different crystal packing states (Fig. 4). Because monomer A in the model of gastrodianin-1 has been refined to the highest degree of precision, its atomic model will accordingly be used in the following descriptions and discussions as a representative of the tertiary structure of the orchid lectin.

Despite being a monomer, gastrodianin resembles the general fold of known bulb lectins, the β-prism II fold established since the first structure of GNA (10) (Fig. 4*b*). It consists of three subdomains (I, II, and III), each of which forms a flat four-stranded β-sheet. A total of 12 β-strands are arranged to form a β-barrel, where a pseudo internal 3-fold axis is located in the center and relates the three faces of the triangular prism. All the strands are perpendicular to the quasi symmetric axis, and consistent with others, quite a number of nonpolar side chains point to the center of the β-barrel (Fig. 5*a*), forming a hydrophobic core stabilized by a network of strong van der Waals interactions. Among these conserved residues are three tryptophan residues, Trp-41, Trp-72, and Trp-104, located in subdomains III, II, and I, respectively (Fig. 5*c*). They are kept invariant through all sequences studied so far (Fig. 1) and believed to play a crucial role in stabilizing the overall fold.

Unique Structural Feature as a Monomer—As expected, the first monomeric model in the monocot mannose-binding lectin superfamily displays some novel structural properties distinct from those observed in known oligomeric structures, mainly in

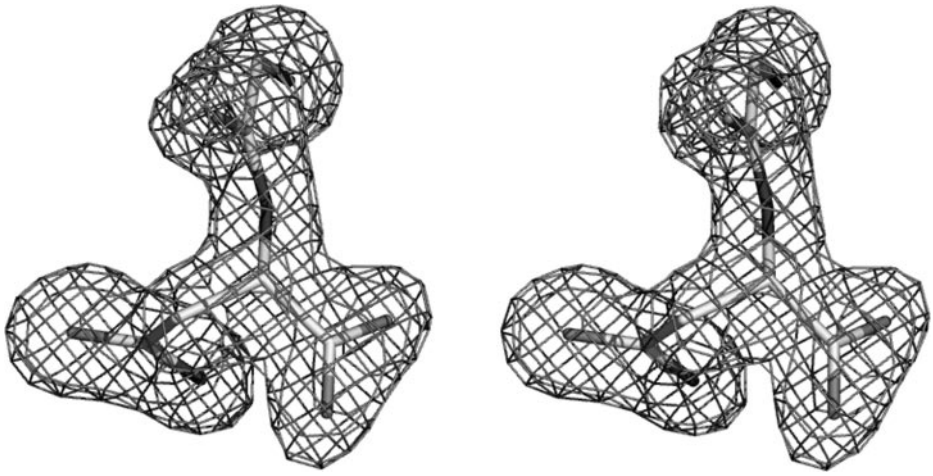

FIG. 2. **Stereo view of the C terminus of molecule A in crystal structure of gastrodianin-1, with the corresponding electron density ($2F_o - F_c$) map contoured at 1.0 σ level.** The carboxyl of Asn-112 at the carboxyl C end of the main chain can be clearly defined.

the structural organization of subdomain I (Fig. 5). In all studied models of bulb lectins, a stable dimer forms a basic structural and functional unit regardless of whether two such dimers further assemble into a tetramer (10, 13) or not (14). A hybrid β-sheet observed in subdomain I of these structures consists of 3 strands (the 1st, 10th, and 11th) from one chain and one (the 12th) from the opposite subunit (Fig. 5*b*). By virtue of this arrangement, a considerable buried surface is given at the dimeric interface, thereby conferring great stability on subunit assembly. This is often referred to as C-terminal exchange in which a *cis* peptide bond between residue 98 and 99, *e.g.* Gly-98 and Thr-99 in GNA, is generally involved (10, 12, 13). Although reasonable links between this unusual peptide bond and the dimerization appear to exist considering its extensive occurrence in this protein superfamily, the definite role has not been understood rigorously.

In principle, however, such a mechanism to exchange the C-terminal peptide does not make any sense in a structure of merolectin, say, gastrodianin. As shown in Fig. 5, within our expectation, the most distinctive feature of the monomeric structure in question lies in subdomain I, where a homogeneous sheet is formed instead of the hybrid one described above. Its 12th strand (residues 102–106) forms an intramolecular sheet together with the 1st (3–5), 10th (84–87), and 11th (92–96) strand from the same chain (Fig. 5, *a* and *b*), providing a structural basis for a stable monomer (Fig. 5*c*). We call it C-terminal self-assembly in contrast to the above C-terminal exchange. Interestingly, the conformation of the C-terminal strand, the 12th, in gastrodianin strictly coincides with its counterpart (residues 101–105) in subunit B of GNA (r.m.s.d. 0.25 Å) if the overall main chain of gastrodianin is superimposed on its subunit C. This guarantees the intactness of the topological invariance of sheet I in gastrodianin model. The hydrophobic core of the β-barrel, hence, also keeps integral and stable in such a fold, especially considering the side chain of Trp-104, which is located in strand 12 and adopts almost the same position and orientation compared with that in other models (Fig. 5*c*). Clearly, such a rearrangement of the C-terminal peptide would bring about a radical decrease or even complete disappearance of the buried surface at the interface between two molecules, which in turn would disallow the orchid lectin to form a dimer like other bulb lectins.

The distinct conformation of 5-residue motif (97–101) of gastrodianin is crucial for the C-terminal self-assembly. In oligomeric lectins only two residues, Gly-98 and Thr-99 (Ser-99 in *A. sativum* agglutinin), present in the corresponding region (Fig. 1) take an unusual *cis* configuration in association with an extended conformation of the following C-terminal peptide 100–109 (Fig. 6*c*). In monomers, *i.e.* gastrodianin, *L. ovata* mannose-binding protein, and *E. helleborine* mannose-binding protein, these two residues are replaced by an aspartic acid and an asparagine residue (labeled with *arrowheads* in Fig. 1) followed by a three-residue insertion (*boxed region* in Fig. 1). Notably, in place of the *cis* peptide bond commonly occurring in oligomeric monocot lectins is a *trans* bond presented at the corresponding site in the refined model of gastrodianin. The short loop of Asp-97–Asn-98–Ser-99–Asn-100–Asn-101 forms a β-turn (Fig. 6*b*) that makes the following C-terminal polypeptide chain flank the 11th strand (Fig. 5*b*) rather than protrude from molecular surface. The β-turn connecting the two strands (the 11th and 12th) close to the C terminus belongs to a 3:5 β-hairpin with a β-bulge inside (Fig. 6*b*) according to the category system of β-hairpins established by Sibanda *et al.* (37). The backbone of the β-hairpin is well stabilized by a local H-bond network mediated by the hydrophilic side chains and three ordered water molecules in this region (Fig. 6*b*). In line with the statistics showing that aspartic acid, asparagine, and serine are the most commonly occurring residues in β-hairpins located at molecular surface of peptides (38), all these residues are presented in this case. From a structural point of view, it is due to the presence of such a β-hairpin arising from residue replacement and insertion in the gastrodianin sequence that the peptide beyond this position has to shift radically from its original location and orientation as in oligomeric states to where it presents in the current model. Consequently, this shift in turn contributes greatly to stabilization of its monomeric state. The unique fold pattern of gastrodianin as a merolectin is observed for the first time (Fig. 5*a*), obviously differing from those of the oligomers reported previously (39) in structural organization of subdomain I, and thus, the structure of gastrodianin should represent a novel type of monomeric monocot mannose-binding lectin.

Structure Determinants and Switch Governing a Quaternary State of Monocot Mannose-binding Lectin—Much effort has gone into the studies of the relationship among sequence motif, structure ,signature and protein oligomerization in several groups of plant lectins for years (2). For instance, legume lectins, exhibiting considerable variations in their oligomeric structures with small changes in their sequences, have been well documented as "natural mutants of quaternary state" (40). Likewise, the superfamily of monocot mannose-binding lectins is also quite heterogeneous in their quaternary organizations despite the high degree of sequence conservation as well as the overwhelming "β-prism II" tertiary fold among all known members. However, information concerning potential sequence elements and structural features that might play crucial roles in

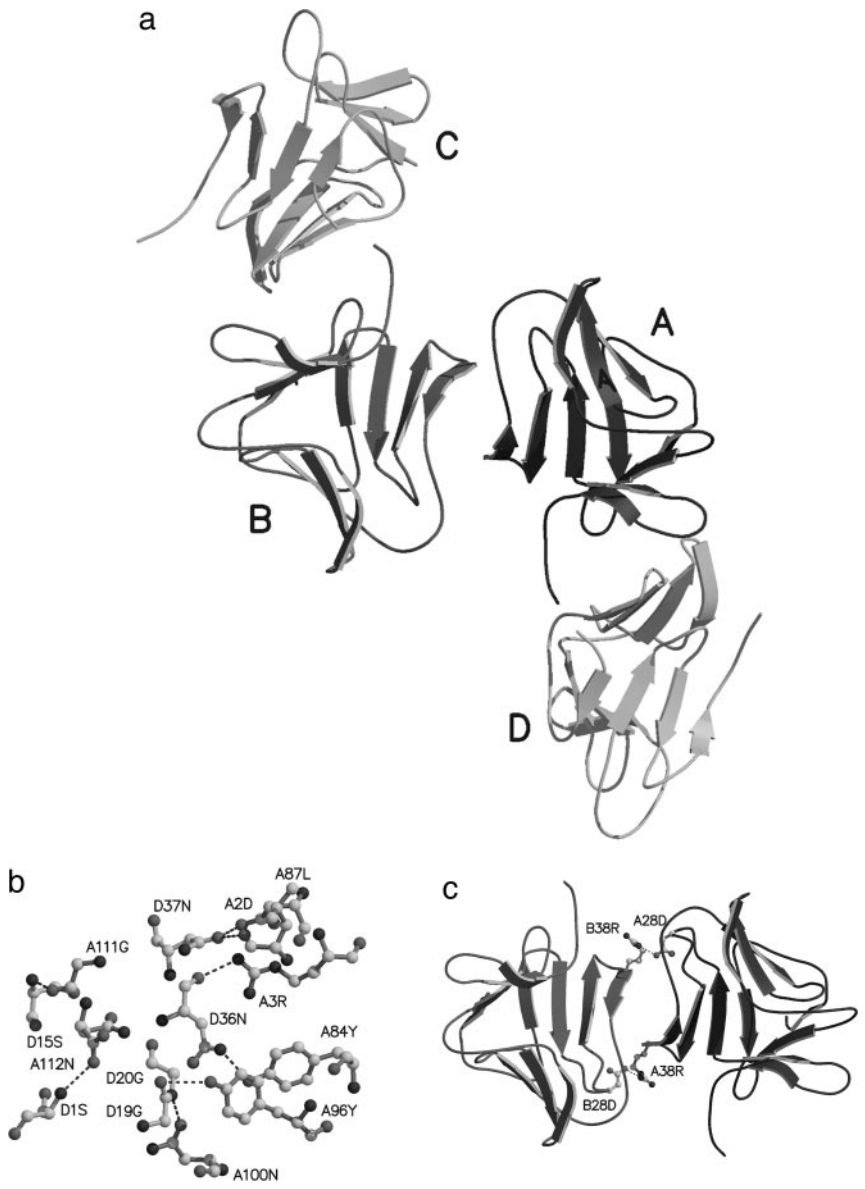

FIG. 3. **The overall structure of gastrodianin-1 in crystals.** *a*, the four independent molecules A, B, C, and D in the asymmetric unit projected down the *y* axis. The pseudo dimer AD and BC are related by a 2-fold non-crystallographic axis approximately parallel to the crystallographic *y* axis. *b*, interactions between monomers A and D. *c*, contacts between A and B.

subunit assembly is still meager. The first monomeric structure availably presented here offers us an opportunity for deeper insight into the main structure determinants governing the protein oligomerization.

Evidently, the architecture of subdomain I of the orchid lectins is the structure determinant for the distinct quaternary state of the monocot mannose-binding lectins. In the case of C-terminal self-assembly, like gastrodianin in the current study, an intramolecular sheet forms in that the 12th strand comes from the intrinsic 10 C-terminal residues of the same polypeptide chain, and the lectin adopts the monomeric state accordingly. Whereas if an intersubunit hybrid sheet is established via C-terminal exchange instead, like GNA and other oligomers, the 12th strand stretches into the partner subunit, and the proteins will fold into dimers or oligomers.

The structural comparison between gastrodianin and the counterpart of GNA shows that the inflection point of the dramatic structure change occurs at position 97 (corresponding to 98 in GNA) (Fig. 6*a*), from which the C-terminal polypeptide chain of monomeric gastrodianin goes into the direction completely different from that of dimeric GNA with a deviation of 131°. This C-terminal peptide can go into either the intramolecular subdomain I or the subdomain I of the partner subunit according to whether it is in a monomeric or oligomeric lectin. The comparison revealed that the distinct configuration of the peptide bond between residues 97 and 98 (corresponding to 98 and 99 of GNA) in association with three-residue insertion or deletion following this dipeptide could be considered as a structural switch for the above structural ramification and, in turn, a determinant of the quaternary state of the monocot mannose-binding lectins. When the crucial peptide bond adopts a normal *trans* conformation associated with the three-residue insertion (Fig. 1), as in the gastrodianin sequence, a five-residue reverse turn belonging to a 3:5 β-hairpin with a β-bulge inside forms (Fig. 6*b*) that renders the following C-terminal segment reversible to contact the flanking peptide chain 11th β-strand of the same subdomain to establish an intramolecular homogenous four-stranded β-sheet (Fig. 5*b*). In contrast, however, if this peptide bond takes an unusual *cis* form instead or a strained conformation with the deletion of three residues in sequences, as the case of GNA (Fig. 6*c*), the followed C-terminal peptide is directed to take an extended conformation and directlyinserts into the subdomain I of the partner subunit to build an intermolecular hybrid β-sheet (Fig. 5*b*) by which dimerization occurs.

It appears notable that the structure switch on monomer/dimmer conversion may be sequence-dependent, as revealed by

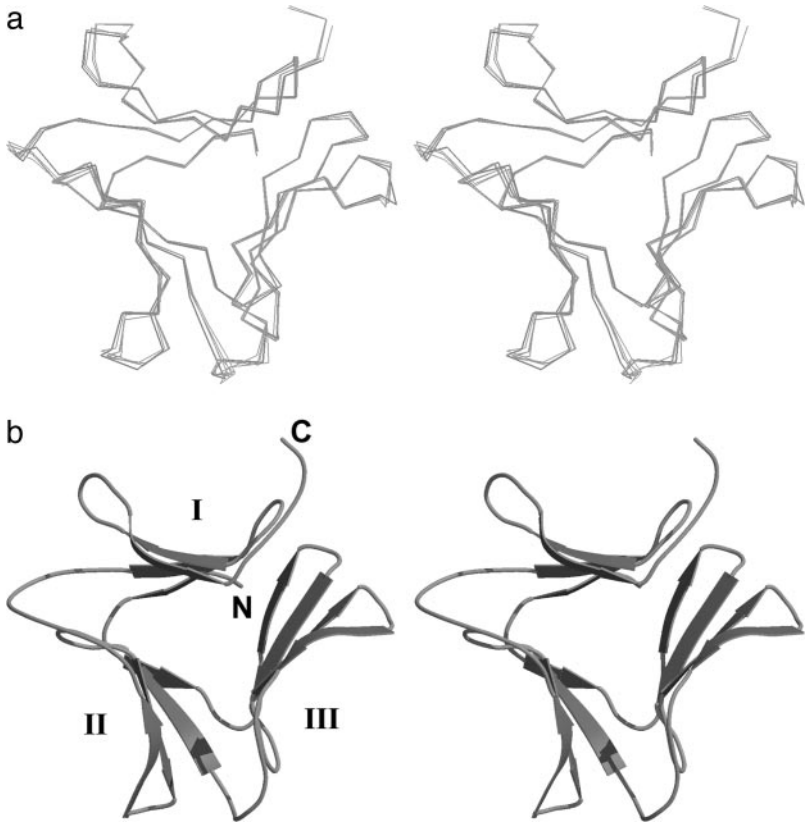

FIG. 4. **Monomeric gastrodianin fold.** *a*, superimpositions between four monomers of gastrodianin-1 and gastrodianin-4 monomer. *b*, the consensus general structure of gastrodianins distinct with three subdomains, I, II, and III, consists of a four-stranded β-sheet, to form β-prism II fold.

sequence alignment with Phi-blast search (41). The five-residue motif, DNSNN, composing the crucial β-hairpin in the gastrodianin model seems to represent a consensus sequence signature occurring in all three known monomers (Fig. 1). To the contrary, in oligomeric structures any side chains at the crucial position (98 in GNA) could be harmful for the *cis*-bond formation with the followed residue because of introducing close contacts, and therefore, glycine is supposed to be the optimum amino acid to be placed at this position. This agrees well with the common occurrence of the two-residue motif G*X* (*X* is any amino acids) in oligomeric sequences (Fig. 1). Taken together with the above statements, these two characteristic motifs existing separately in monomers or oligomers can be considered as sequence determinants that govern the quaternary states of monocot mannose-binding lectins.

The fine structure of gastrodianin in comparison with those of other bulb lectins in oligomeric state uncovers a structural mechanism by which the distinct quaternary states of monocot mannose-binding lectins could be governed, as shown in Fig. 6*d*. The observations also manifested a special way to achieve the distinct quaternary state of proteins through the strained backbone geometry.

The Mutation Experiment Confirming the Structure Determinant on Protein Oligomerization—To confirm the main conclusion from structural analysis regarding quaternary organization of bulb lectins, a mutation experiment was performed. Because satisfying results have never been achieved in our efforts to obtain soluble recombinant gastrodianin from several *E. coli* and yeast expression systems, expression of MBP-gastrodianin-1 fusion protein in *E. coli* was established (see "Materials and Methods"). Subsequently, a mutagenesis was designed on this fusion gene, with the loop from 97 to 101 addressed first. Asp-97 and Asn-98 were mutated into glycine and threonine residues, respectively, whereas the codon of Ser-99, Asn-100, and Asn-101 was deleted from the gene to match the sequence of GNA in this segment.

After expression and purification, recombinant fusion proteins with high purity of the wild type and the mutant were both applied to gel filtration chromatography to compare their molecular sizes in solution. On the elution profile from Superdex 75 column, the peak of native MBP-gastrodianin appeared at the elution volume 10.1 ml (the expected time of 20.2 min) corresponding to an apparent molecular weight of about 53 (Fig. 7*A*), which is generally consistent with the monomeric molecular size of the recombinant fusion protein (43 and 13 kDa for MBP and gastrodianin, respectively). The mutant, however, was eluted in the flow-through fraction with the elusion volume of 8.2 ml (the expected time of 16.4 min) (Fig. 7*C*), indicating its molecular size must be greater than 70 kDa. On the elution profile from Superdex 200 column, the peak of mutant MBP-gastrodianin was eluted at the elution volume of 13.4 ml (the expected time of 26.8 min), corresponding to an apparent molecular weight of about 130 (Fig. 7*E*), which is roughly coincident to the molecular size of a dimeric form of the muted fusion protein. The SDS-PAGE analyses of the elution peaks of the wild type and the mutant fusion protein are shown in Fig. 7, *B* and *D*, respectively, which clearly identify the results from the chromatography. These results unquestionably confirm the change of the protein quaternary states caused by mutation, and most likely the association form of the mutant fusion protein can be assumed as dimerization. From these experimental data we can sensibly conclude that this sequence motif from position 97 to 101 is responsible for the conversion between the monomeric and dimeric states of monocot mannose-binding lectins.

Putative Carbohydrate Binding Sites—Although the complex structure of gastrodianin with its saccharide ligands was not available in our studies, some binding features can also be anticipated by comparison with its homologous sequences and structures. The consensus sequence motif Q*X*DXN*X*V*X*Y (*X* is

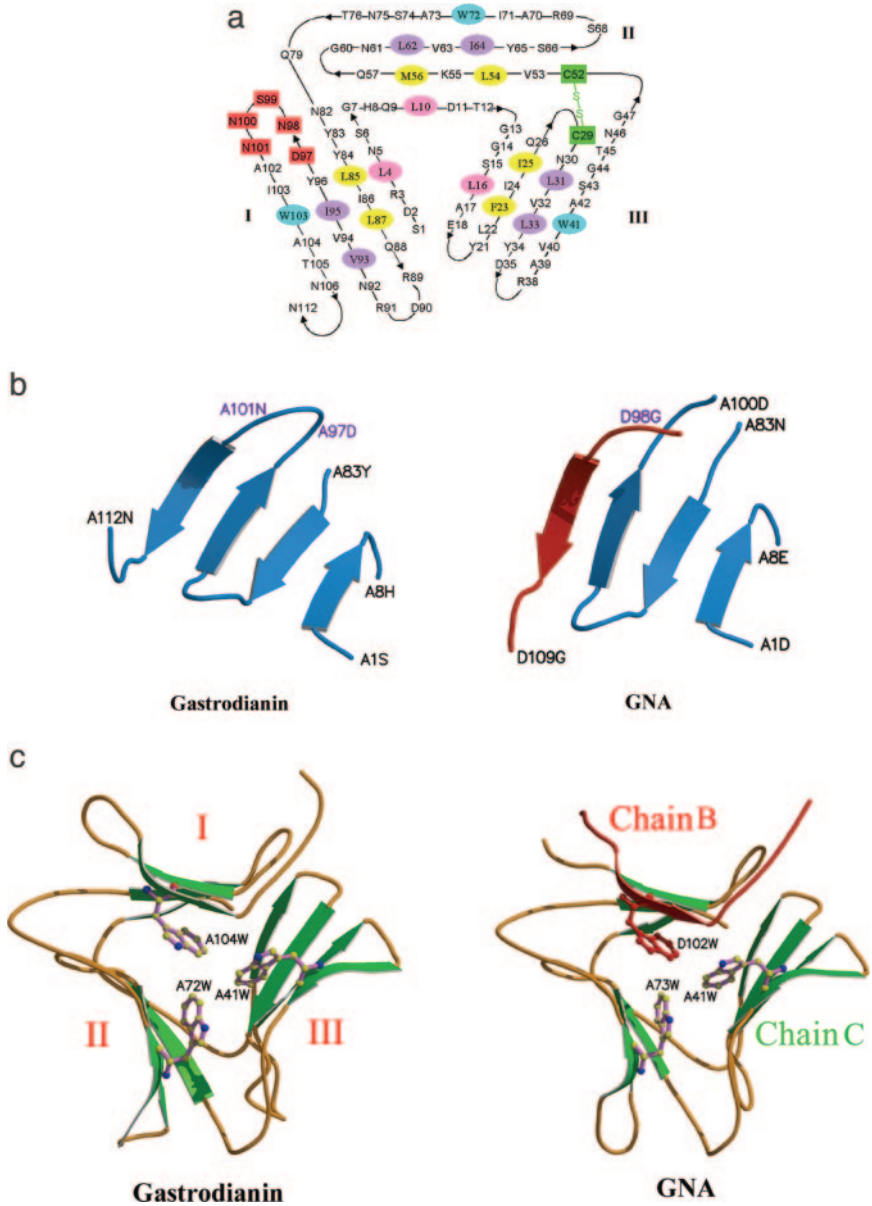

FIG. 5. **Structural organization of subdomain I in monomeric gastrodianin through the C-terminal self-assembly in comparison with that of GNA via the C-terminal exchange.** *a*, unique fold pattern of gastrodianin. Subdomain I composed of the four-stranded β-sheet from a single chain is the structural basis for its monomeric form. Hydrophobic residues that form the hydrophobic core inside the barrel are colored *pink*, *yellow*, *purple*, and *cyan* according to their strand location. The single disulfide bridge is shown in *green*. Residues in a reverse turn from 97 to 101 that determines the fold of the C-terminal strand are *highlighted* with a magenta background. *b*, the homologous (*left*) and hybrid (*right*) four-stranded β-sheets appeared in the monomeric gastrodianin and dimeric GNA subunit, respectively. *c*, architectural comparison of the protomer between gastrodianin (*left*) and GNA (*right*), whose subdomain I was built in the mode of C-terminal self-assembly and C-terminal exchange, respectively. For the C-terminal self-assembly, all the four β-strands composing the subdomain I come from the same chain (*left*), whereas for the C-terminal exchange (*right*) the last β-strand (*red*) with the residue Trp-102 is located on the external chain from the opposite subunit. The GNA models was drawn from PDB entry 1JPC.

one of any amino acid residues) (5) occurs in all three putative carbohydrate recognition domains of the orchid protein (Fig. 1), indicating the same binding mode as other bulb lectins. The conserved side chains in the binding pockets of gastrodianin coincide well with those in GNA (r.m.s.d. 0.17 Å), strengthening the view that binding carbohydrate does not cause any noticeable conformational change of the protein itself. This also confirms its strong preference of the axial hydroxyl at position 2 in the ligand, which is the common property shared with all known members in this protein superfamily (10, 13, 14). However, such a deduction may lead to a variance from previous biochemical observations, suggesting another possibility of chitin binding activity of the orchid lectin (23).

Despite the similar geometries at binding sites in both the orchid and snowdrop lectins, their preferences to complex glycans may vary considerably. Previous observations have suggested that the variability in quaternary structures may be an alternative means of diversifying ligand preferences among lectins (42). A good example for bulb lectins has been well documented. Some tetramers such as GNA or *N. pseudonarcissus* lectin display an inhibitory activity against retrovirus resulting from their strong affinity to GP120, the major glycoprotein of human immunodeficiency virus (6, 7), whereas the garlic agglutinin, a dimer, does not (9). The structure of the snowdrop lectin complex with a branched mannopentaose revealed two distinct binding modes, both cross-linking two subunits to form extended binding sites (43). Gastrodianin, however, obviously cannot dock the mannopentaose in a similar fashion considering its monomeric state. In contrast, one can hardly believe that a monomer like gastrodianin is able to bind polysaccharide with complicated branches as do oligomers, due to a lack of contacts from neighboring subunits. This may lead one to surmise that the orchid lectin possesses a distinct choice for its ligands, which is most probably different from what we know for oligomers.

Biological Implications—Like other lectin families, the physiological role of the monocot mannose binding lectins remains poorly understood thus far (2) even though this question has been addressed since the first discovery of GNA (44). As evidenced in recent years, bulb lectins are gradually believed to serve as a device of the plant defense system against the ravage of rodent pests, insects, and microorganisms (1, 8). For instance, the presumed protective role of GNA has been well established from experiments in which the detrimental effect

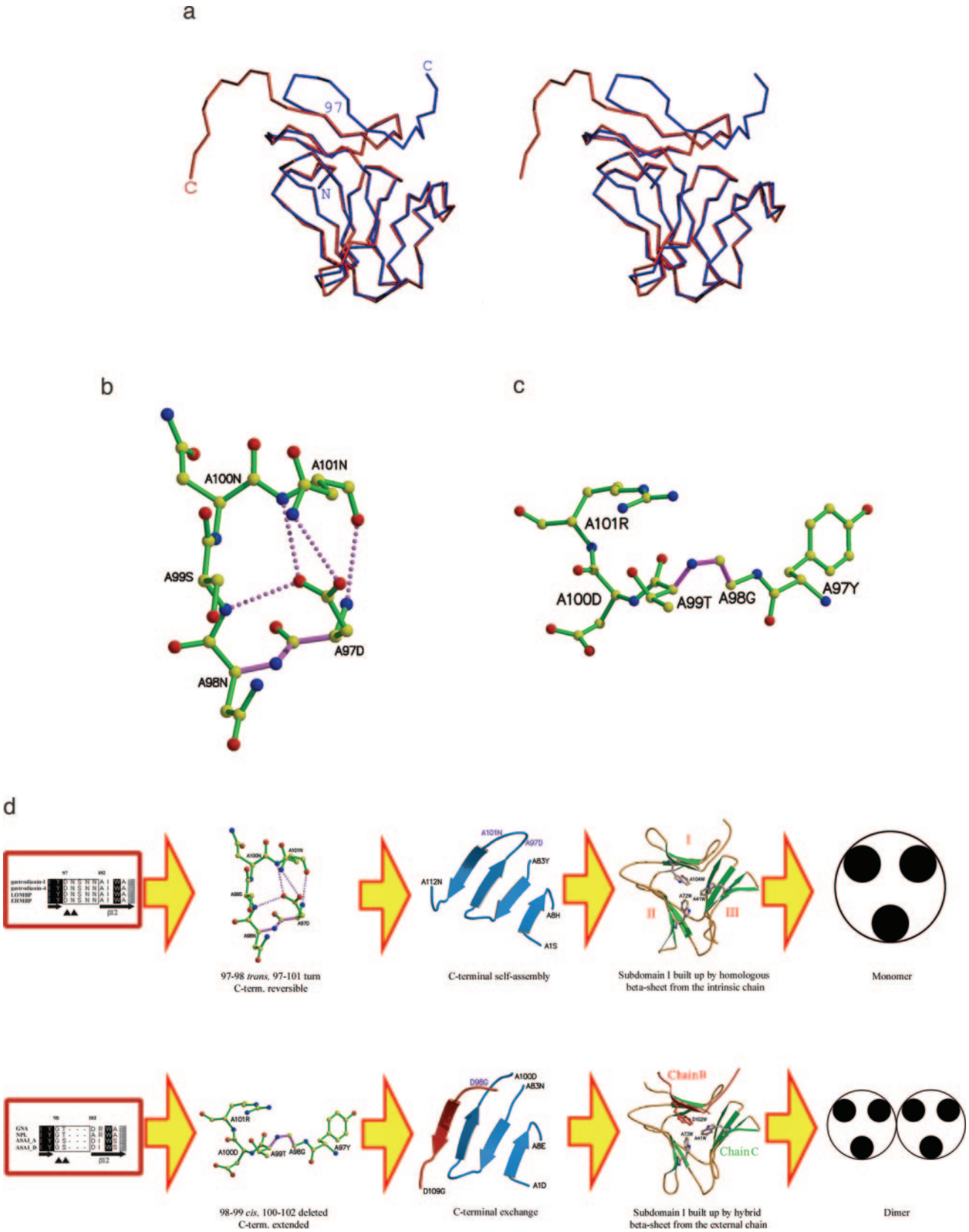

FIG. 6. **Structural switch for the monomer/dimer conversion.** *a*, the structural comparison between gastrodianin (*blue*) and the counterpart of GNA (*red*). An inflection point of the dramatic structure change appeared at position 97 (corresponding to 98 in GNA) from which the C-terminal polypeptide chains go into complete different directions with a deviation of 131°. *b*, the 5-residue reverse turn (97–101) formed in gastrodianin. In the turn the peptide bond (97–98) adopts a usual *trans* form, and the reversed conformation is well stabilized with a hydrogen bond network, which directed the C-terminal segment to turn into the intrinsic subdomain I to form the homologous β-sheet through the C-terminal self-assembly. *c*, the extended conformation in the corresponding region of GNA caused by an unusual *cis* peptide bond between the corresponding residues 98 and 99, which induced the C-terminal peptide to go into subdomain I of its partner subunit to build up a hybrid β-sheet with C-terminal exchange. *d*, the two modes schematically showing the structural mechanisms by which the quaternary states of monocot mannose-binding lectins could be governed.

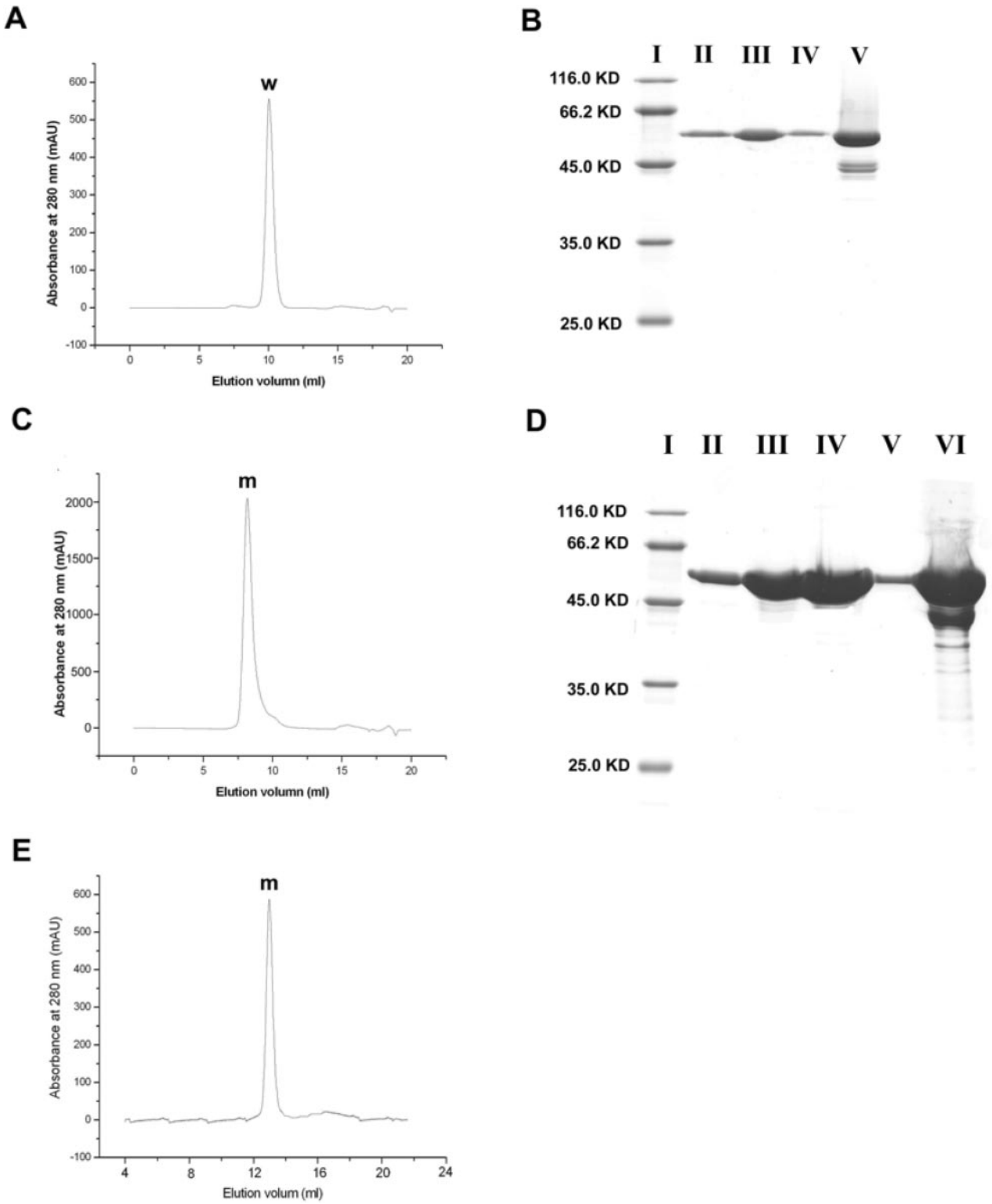

FIG. 7. **The elution profiles from size exclusion chromatography and SDS-PAGE results of the native (*A* and *B*) and mutant fusion proteins (*C*, *D*, and *E*).** *A*, Superdex 75 column for the wild type fusion protein. The native fusion protein appeared at peak *w* with the elution volume of 10.1 ml (expected time of 20.2 min) corresponding to an apparent molecular weight of 53. *B*, SDS-PAGE results of the recombinant native fusion protein. *Line I* is the standard protein marker; *line V* represents the elution peak after affinity chromatography; l*ine II*~*IV* are the fractions of whole peak w in *A*, which show that the elution of Superdex 75 column has only one fraction with a molecular weight of 55, estimated from BandScan 4.5 software. *C*, Superdex 75 column for the mutant fusion protein. The mutant protein in question was eluted in the flow-through fraction with the elusion volume of 8.2 ml (expected time of 16.4 min) (*C*), indicating its molecular size must be greater than 70 kDa. *D*, SDS-PAGE result of the mutant fusion protein. *Line I* is the standard protein marker; *line VI* represents the elution peak after affinity chromatography; *Line II*~*V* are the fractions of whole peak *m* in *C*, which shows a molecular weight of about 55 (estimated from BandScan 4.5 software). *E*, elution profile of the mutant protein from Superdex 200 column. The mutant fusion protein appeared at peak *m* with the elution volume of 13.4 ml (expected time of 26.8 min), corresponding to an apparent molecular weight of about 130, which is roughly coincident to the molecular size of a dimeric form of the muted fusion protein. The result indicated that the mutant fusion protein should consist of two identical mutant protomers linked by non-covalent interactions. These results confirm the change of the protein quaternary states caused by mutation and, most likely, the association form of the mutant fusion protein can be assumed as dimerization.

on sucking invertebrates was demonstrated when they were fed with artificial diets containing the lectin or transgenic plants expressing its gene (45, 46). Likewise, gastrodianin has been thought to be involved in microorganism defense and was first defined as an antifungal protein (20, 22). The orchid *G. elata*, unlike green plants, lives on the released nutrients from harvested hypha rather than leading an autotrophic life. Gastrodianin, in this circumstance, seems to exist as a long term evolutional product of such specialization, which helps the plant fight with its symbiotic partner, the fungi. From an evolutionary point of view, it possibly follows that nature has evolved monocot mannose-binding lectins with different quaternary states for their adaptation in various situations. Whereas the oligomers, such as GNA and *N. pseudonarcissus* lectin, play a defensive role against insects or other invertebrates, the monomers function as antifungal proteins.

In past decades formidable arrays of plant proteins have been identified as antifungal proteins, and a number were, hence, biotechnologically applied in crop production, including chitinases (47), hevein-type proteins (48, 49), thionins, plant defensins (50), and type-1 ribosome-inactivating proteins (51). Exclusively, gastrodianin belongs to none of the known classes of antifungal proteins in terms of sequence homology or structure similarity, although its inhibitory activity against the fungus *V. ambiens* is on a par with that of another established antifungal lectin, *Urtica diocia* agglutinin (49). Despite the fact that most plant lectins with antifungal properties are found to be chitin-binding proteins, such as hevein or hevein-like proteins, we can hardly believe that the orchid lectin works in the same manner because its binding specificity seems to be fixed on mannose only from our structure studies as a typical monocot mannose-binding lectin. Noticeably, however, the most important feature of the orchid protein mainly lies in its particular quaternary state, distinctive from other known members in the superfamily of bulb lectins, and in this way, the antifungal activity of gastrodianin appears to arise more from its overall structure as a monomer than from any local structure variations. We thus conclude that it is the monomeric form that plays the dominant role in its inhibitory ability. This view is supported by an observation that a homologous merolectin from the orchid *E. helleborine* also retards hyphal growth *in vitro*, whereas related dimeric or tetrameric lectins, including GNA, do not display any antifungal activities (25). In principle, a smaller molecular size, as a result of its monomeric form, definitely favors the orchid lectin in penetrating through fungal cell walls, since the size exclusion limit for a typical antifungal protein stays around 15–20 kDa (52). This evidence comes from the bioassay of the MBP-gastrodianin fusion protein that shows no inhibitory activity *in vitro*, as opposed to the protease-cleaved protein (25).

Even with such speculation, the details of how gastrodianin resists fungal invasion remains unclear because of our meager knowledge about the cell wall structure of the fungus *A. mellea*, the symbiotic partner with the orchid *G. elata*. A scenario that one can consider concerns the carbohydrate binding preference of the orchid lectin. The lectin may work in such a way that, like chitin-binding proteins, it binds mannose-rich glycans, which are used by phytopathogenic fungi as building blocks in their cell wall constructions and consequently block their hyphal growth. Alternatively, gastrodianin can also bind mannose-containing glycoconjugates on fungal membranes so as to affect their cellular metabolism thereafter, which is implied by homology modeling of the core domain of the endogenous lectin comitin from *Dictyostelium discoideum* using GNA as the template, showing its mannose binding specificity on mannose residues in membrane glycans (53).

Acknowledgments—The x-ray data collection was supported by High Energy Accelerator Research Organization of Japan Grant 2002G310. We thank Prof. N. Sakabe for help during data collection.

REFERENCES

1. Peumans, W. J., and Van Damme, E. J. (1995) *Plant Physiol.* **109,** 347–352
2. Van Damme, E. J. M., Peumans, W. J., Barre, A., and Rouge, P. (1998) *Crit. Rev. Plant Sci.* **17,** 575–692
3. Van Damme, E. J. M., Allen, A. K., and Peumans, W. J. (1988) *Physiol. Plant* **73,** 52–57
4. Van Damme, E. J., Astoul, C. H., Barre, A., Rouge, P., and Peumans, W. J. (2000) *Eur. J. Biochem.* **267,** 5067–5077
5. Ramachandraiah, G., and Chandra, N. R. (2000) *Proteins* **39,** 358–364
6. Balzarini, J., Schols, D., Neyts, J., Van Damme, E., Peumans, W., and De Clercq, E. (1991) *Antimicrob. Agents Chemother.* **35,** 410–416
7. Marchetti, M., Mastromarino, P., Rieti, S., Seganti, L., and Orsi, N. (1995) *Res. Virol.* **146,** 211–215
8. Barre, A., Van Damme, E. J., Peumans, W. J., and Rouge, P. (1996) *Plant Physiol.* **112,** 1531–1540
9. Dam, T. K., Bachhawat, K., Rani, P. G., and Surolia, A. (1998) *J. Biol. Chem.* **273,** 5528–5535
10. Hester, G., Kaku, H., Goldstein, I. J., and Wright, C. S. (1995) *Nat. Struct. Biol.* **2,** 472–479
11. Chantalat, L., Wood, S. D., Rizkallah, P. J., and Peynolds, C. D. (1996) *Acta Crystallogr. D Biol. Crystallogr.* **52,** 1146–1152
12. Wood, S. D., Wright, L. M., Reynolds, C. D., Rizkallah, P. J., Allen, A. K., Peumans, W. J., and Van Damme, E. J. (1999) *Acta Crystallogr. D Biol. Crystallogr.* **55,** 1264–1272
13. Sauerborn, M. K., Wright, L. M., Reynolds, C. D., Grossmann, J. G., and Rizkallah, P. J. (1999) *J. Mol. Biol.* **290,** 185–199
14. Chandra, N. R., Ramachandraiah, G., Bachhawat, K., Dam, T. K., Surolia, A., and Vijayan, M. (1999) *J. Mol. Biol.* **285,** 1157–1168
15. Ramachandraiah, G., Chandra, N. R., Surolia, A., and Vijayan, M. (2002) *Acta Crystallogr. D Biol. Crystallogr.* **58,** 414–420
16. Wright, L. M., Reynolds, C. D., Rizkallah, P. J., Allen, A. K., Van Damme, E. J., Donovan, M. J., and Peumans, W. J. (2000) *FEBS Lett.* **468,** 19–22
17. Bachhawat, K., Kapoor, M., Dam, T. K., and Surolia, A. (2001) *Biochemistry* **40,** 7291–7300
18. Van Damme, E. J., Balzarini, J., Smeets, K., Van Leuven, F., and Peumans, W. J. (1994) *Glycoconj. J.* **11,** 321–332
19. Van Damme, J. M., Smeets, K., Torrekens, S., Van Leuven, F., and Peumans, W. J. (1994) *Eur. J. Biochem.* **221,** 769–777
20. Hu, Z., and Huang, Q. Z. (1994) *Acta Bot. Yunnanica* **16,** 169–177
21. Yang, Z., and Hu, Z. (1990) *Acta Bot. Yunnanica* **12,** 421–426
22. Jiang, L., Xu, J. T., Wang, H., Liu, H. X., and Sun, Y. R. (1993) *Acta Bot. Sin.* **35,** 593–599
23. Xu, Q., Liu, Y., Wang, X. C., Gu, H., and Chen, Z. L. (1998) *Plant Physiol. Biochem.* **36,** 899–905
24. Hu, Z., Huang, Q. Z., Liu, X. Z., and Yang, J. B. (1999) *Acta Bot. Yunnan* **21,** 131–138
25. Wang, X., Bauw, G., Van Damme, E. J., Peumans, W. J., Chen, Z. L., Van Montagu, M., Angenon, G., and Dillen, W. (2001) *Plant J.* **25,** 651–661
26. Wang, X. C., Diaz, W. A., Bauw, G., Xu, Q., Montagu, M. V., Chen, Z. L., and Dillen, W. (1999) *Acta Bot. Sin.* **41,** 1041–1045
27. Liu, W., Hu, Y. L., Wang, M., Xiang, Y., Hu, Z., and Wang, D. C. (2002) *Acta Crystallogr. D Biol. Crystallogr.* **58,** 1833–1835
28. Otwinowski, Z., and Minor, W. (1997) *Methods Enzymol.* **276,** 307–326
29. Navaza, J. (1994) *Acta Crystallogr. Sect. A* **42,** 140–149
30. Vagin, A., and Teplyakov, A. (2000) *Acta Crystallogr. D Biol. Crystallogr.* **12,** 1622–1624
31. Collaborative Computational Project, N. (1994) *Acta Crystallogr. D Biol. Crystallogr.* **50,** 760–763
32. Jones, T. A., and Kieldgaard, M. (1993) *O*, Version 5.9, The manual, Uppsala University, Uppsala, Sweden
33. Brunger, A. T., Adams, P. D., Clore, G. M., DeLano, W. L., Gros, P., Grosse-Kunstleve, R. W., Jiang, J. S., Kuszewski, J., Nilges, M., Pannu, N. S., Read, R. J., Rice, L. M., Simonson, T., and Warren, G. L. (1998) *Acta Crystallogr. D Biol. Crystallogr.* **54,** 905–921
34. Murshudov, G. N., Vagin, A. A., and Dodson, E. J. (1997) *Acta Crystallogr. D Biol. Crystallogr.* **53,** 240–255
35. Vagin, A. A., Richelle, J., and Wodak, S. J. (1999) *Acta Crystallogr. D Biol. Crystallogr.* **55,** 191–205
36. Laskowski, R., MacArthur, M., Moss, D., and Thornton, J. (1993) *J. Appl. Crystallogr.* **26,** 283–291
37. Sibanda, B. L., Blundell, T. L., and Thornton, J. M. (1989) *J. Mol. Biol.* **206,** 759–777
38. Blanco, F., Ramirez-Alvarado, M., and Serrano, L. (1998) *Curr. Opin. Struct. Biol.* **8,** 107–111
39. Hester, G., and Wright, C. S. (1996) *J. Mol. Biol.* **262,** 516–531
40. Srinivas, V. R., Reddy, G. B., Ahmad, N., Swaminathan, C. P., Mitra, N., and Surolia, A. (2001) *Biochim. Biophys. Acta* **1527,** 102–111
41. Altschul, S. F., Madden, T. L., Schaffer, A. A., Zhang, J., Zhang, Z., Miller, W., and Lipman, D. J. (1997) *Nucleic Acids Res.* **25,** 3389–3402
42. Drickamer, K. (1995) *Nat. Struct. Biol* **2,** 437–439
43. Wright, C. S., and Hester, G. (1996) *Structure* **4,** 1339–1352
44. Van Damme, E. J. M., Allen, A. K., and Peumans, W. J. (1987) *FEBS Lett.* **215,** 140–144
45. Hilder, V. A., Powell, K. S., Gatehouse, A. M. R., Gatehouse, J. A., Gatehouse, L. N., Shi, Y., Hamilton, W. D. O., Merryweather, A., Newell, C., Timans, J. C., Peumans, W. J., Van Damme, E. J. M., and Boulter, D. (1995) *Transgenic Res.* **4,** 18–25
46. Rahde, Y., Sauvion, N., Febvay, G., Peumans, W. J., and Gatehouse, A. M. R.

(1995) *Entomol. Exp. Appl.* **76,** 143–155
47. Schlumbaum, A., Mauch, F., Vögeli, U., and Boller, T. (1986) *Nature* **324,** 365–367
48. Van Parijs, J., Broekaert, W. F., Goldstein, I. J., and Peumans, W. J. (1991) *Planta* **183,** 258–262
49. Van Parijs, J., Joosen, H. M., Peumans, W. J., Genus, J. M., and Van Laere, A. J. (1992) *Arch. Microbiol.* **158,** 19–25
50. Terras, F. R., Schoofs, H. M., De Bolle, M. F., Van Leuven, F., Rees, S. B., Vanderleyden, J., Cammue, B. P., and Broekaert, W. F. (1992) *J. Biol. Chem.* **267,** 15301–15309
51. Leah, R., Tommerup, H., Svendsen, I., and Mundy, J. (1991) *J. Biol. Chem.* **266,** 1564–1573
52. Raikhel, N. V., Lee, H. I., and Broekaert, W. F. (1993) *Annu. Rev. Plant Physiol. Plant Mol. Biol.* **44,** 591–615
53. Barre, A., Van Damme, E. J., Peumans, W. J., and Rouge, P. (1999) *Plant Mol. Biol.* **39,** 969–978
54. Luzzati, P. V. (1952) *Acta Crystallogr. D Biol. Crystallogr.* **5,** 802–810
55. Cruickshank, D. W. (1999) *Acta Crystallogr. D Biol. Crystallogr.* **55,** 583–601